(Received 19 June 2025, Accepted 22 September 2025, Scheduled 22 October 2025)

Investigation of Rectangular Dielectric Resonator MIMO Antenna with Modes for 5G-Millimeter-Wave Applications

Garima Sharma* and Mithilesh Kumar

Department of Electronics Engineering, Rajasthan Technical University, Kota, Rajasthan, India

ABSTRACT: A four-port cross-shaped RDRA multiple-input-multiple-output antenna is proposed for 5G millimeter-wave applications. The present investigation targeted the 5G n257 band (26.5–29.5 GHz) with resonance exactly at 28.5 GHz. The proposed DR MIMO antenna is constructed over roger RT duroid 5880 laminates with the floor area $10.4 \times 10.4 \times 0.254\,\text{mm}^3$ with the compact DRA of dimension $7.6 \times 7.6 \times 1.5\,\text{mm}^3$. Each element of the DRA is fed by a conformal fed microstrip line that generates $TE_{21\partial}$, $TE_{41\partial}$, $TE_{11\partial}$, $TM_{14\partial}$, and $TM_{41\partial}$ modes. The symmetricity of the structure is maintained by locating four arms of the DRA at a separation of 90°, which generates omnidirectional radiation pattern and offers good radiation diversity. The proposed antenna offers 14% impedance bandwidth with below −15 dB isolation. Following the thorough simulation procedure, it has been verified that the compact MIMO DRA operates exactly at 28.5 GHz. To validate design, a four-port single element DRA operating at 28.5 GHz was simulated in CST studio suite, fabricated via ceramic material and then measured in an anechoic chamber. The proposed antenna shows the peak gain of 8.4 dBi with 74% radiation efficiency. Both simulation and measurement observations are used to examine MIMO parameters. The Envelope Correlation Coefficient is reported as 0.0125, and Diversity Gain is reported as 9.8 in approximately all the cases. The Total Active Reflection Coefficient is found to be 18% at 28.5 GHz in measurement and 18.5% at 28.5 GHz in simulation.

1. INTRODUCTION

A successful transmission technique employed in contemporary wireless communication is called Multiple Input Multiple Output (MIMO). MIMO, as the name suggests, combines transmission and reception using multiple antennas. Increased data rate and system efficiency are facilitated by the combination of various transmission sources. Because MIMO antennas can give a larger data rate without increasing power levels, they constitute the foundation of today's wireless communication systems [1]. The market of wireless data communication is projected to grow from USD 1.63 billion in 2024 to USD 4.85 billion by 2032, exhibiting a compound annual growth rate (CGAR) of 14.56% during the forecast period (2024–2032) [1]. The increased need for a powerful network has resulted in the rise of internet services that include 3G, 4G, 5G, and 6G networks, high speed internet services, increased technological advancement in mobile communication, shift towards IOT, digital transformation across industry, telecommunication market demands, public-private partnership, smart cities which are the key markets drivers contributing to market growth and expansion. This requires high data rate, fast speed, and large bandwidth. The multiple devices are required to be connected with the same nodal point. A number of antennas have been developed to meet these requirements. A number of comparable radiators are positioned on the same substrate in a MIMO antenna. A Dielectric Resonator Antenna (DRA), microstrip, or slot radiator could be these radiators. Because DRAs can provide great efficiency of radiation and gain at high frequencies, they are the most efficient of them [2].

The IOT (Internet of Things), mobile internet, autonomous vehicles, and virtual reality are currently developing at previously unheard of speeds. These technologies require vast exchanges of information and require very fast data rates and large capacities. As a result, the future fifth-generation mobile communication systems may opt to use the mm-wave spectrum. The present investigation targeted the 5G n257 band (26.5–29.5 GHz) in mm-wave spectrum. Here, the Signal to Interference and Noise Ratio (SINR) is significantly reduced by the high attenuation and path loss associated with EM (electromagnetic) wave propagation in the millimeter wave range. In order to address the issue, 5G networks are anticipated to employ mm-wave MIMO technology [3]. As a result, integrating many antennas in a limited space becomes a critical problem. Due to inadequate isolation, the performance of the system will be negatively impacted when two or more antennas are positioned close to one another [4]. Thus, throughout the last ten years, an extensive amount of research has been focused on improving gain and bandwidth, achieving adequate isolation and reducing mutual coupling between antenna elements.

Metallic antennas are used from the pristine time but fail to satisfy the requirement at high frequencies due to narrow bandwidth, conductor losses, low efficiency, and high level of cross polarization. To mitigate these issues, dielectric resonator antennas are investigated, particularly at mm-wave frequency bands. DRAs use dielectric material (non-conducting) to resonate at specific frequencies. DRA offers attractive features like high efficiency, wide bandwidth, availability of vari-

* Corresponding author: Garima Sharma (garima.phd21@rtu.ac.in).

ous geometries, different feeding mechanisms, and good power handling capacity. It possesses design flexibility and versatility. Rectangular DRA has two degrees of freedom in terms of width to height and height to length ratios, making it preferable for mm-wave applications. Therefore, rectangular shape DRA is commonly used as compared to cylindrical or hemispherical ones [2].

DRA is an open resonating antenna which is fabricated from low-loss dielectric material that is ceramic in this work. DRA offers several advantages like small size for high frequency, a flexible feeding technique, high efficiency, and wideband. DRA is having the ability to radiate in both linear and circular polarizations [5].

Since permittivity and dielectric resonator dimension are inversely related, or small size of DR is ideal for high permittivity, according to reports, when permittivity is taken ≥ 9, radiation efficiency is more than 75% [3]. The rapid growth of mobile wireless communication industry has a demand for wide coverage area and high data rate. In order to meet these requirements, MIMO antennas have been developed. For achieving good diversity performance and enhanced spectral efficiency, MIMO antennas are chosen. It can achieve high bit rate with the help of multiple antennas at transmitter and receiver sides.

Data on radiated fields, bandwidth, Q-factor (radiation quality), the field distribution, and resonant frequency inside the resonator are all useful to characterize the design of DRA [5]. In DRA, the primary form of excitation is based upon the feeding methods employed, as well as the feeding or source point. To power a DRA at millimeter wave frequency bands and in accordance with research requirements, a variety of feeding systems are employed, including microstrip line, aperture coupled, coaxial probe, and conformal fed transmission lines. The high efficiency and wide bandwidth of DRA make it the ideal antenna for 5G mm-wave frequency bands. The lack of conduction losses is one of DRAs' inherent qualities. Due to this characteristic, DRAs are excellent choices for high-frequency applications.

A multi-polarized antenna design with a finite size and the ability to increase capacity can also be customized using the multi-polarization feature of MIMO technology. There may be a space constraint problem when integrating multiple antennas onto a small device. Thus, the alternate approach is a single element MIMO antenna. Researchers are examining various Dielectric Resonator (DR) shapes in conjunction with radiation properties including excitation systems in the context of MIMO with DR elements, in a recent development [6]. Within a limited bandwidth and power level, MIMO antennas at the transmitter and reception ends improve linking ability and dependability. DRAs are effective since they do not have any conduction losses. On the other hand, these antennas result in excellent radiation characteristics, superior gain, and smooth excitation [7]. Thus, a high frequency MIMO antenna that incorporates DR elements into its design will have an added benefit above other standard topological antennas. DR MIMO can thereby address the issue of reduced radiation performance near the antenna array. By adjusting the DR element's size, wide frequency range can be guaranteed. Using a DR element in an antenna allows for multiband or wide coverage [8]. High permittivity material DRA has electrically minimal gain in radiation efficiency and bandwidth. In comparison to other traditional antennas, DRA excitation technique is much simpler. For DR MIMO antenna design to achieve sufficient port isolation, the decoupling association must be correctly matched [9].

Rectangular type DR elements are superior because they have greater shape-changing flexibility, which allows them to control the antenna's impedance bandwidth and diversity performance. Although the introduction of MIMO antennas with DR elements offers several benefits, MIMO designs nevertheless require a high degree of isolation between the antenna ports.

The benefits of the DR antenna include its compact size, broad bandwidth, and simplicity in excitation methods. Furthermore, at mm-wave frequency, the DRA's loss is made quite small because it is built entirely of dielectric. DRA is a great antenna option for millimeter-wave systems due to all of these attributes. Orthogonal feed placement is another crucial method for achieving acceptable isolation in DR MIMO antennas without the need for additional decoupling structures. Feed networks have been employed to achieve extremely high port isolation in the present literature. Two orthogonal feed lines are combined to form each feed network. These benefit achieving a good gain of isolation in the suggested MIMO DRA.

Antenna with pattern diversity having broadside radiation pattern finds interesting application in mm-wave communication. The different types of pattern diversity DR antennas have been designed [4, 5]. An 8-port MIMO DRA is proposed to minimize Envelope Correlation Coefficient (ECC) from 0.167 to 0.037 by using reflector element, but it occupies large space and uses bidirectional pattern diversity.

Many researchers have explored different shapes of DRA at millimeter wave frequency bands [6]. Pan et al. presented a facile technique for decoupling utilizing metallic vias to enhance the isolation in a 1×2 MIMO DRA. The antenna comprises the frequency range of 26 GHz in both the planes. It offers an isolation up to 30 dB only [7]. Ref. [8] proposes a MIMO DRA in between the frequency range 27.5–28.35 GHz. It offers the minimum isolation of 12 dB. Many technologies have been developed to improve MIMO DRA isolations. They include metasurface designs, Frequency Selective Surfaces (FSSs), hybrid feeding mechanisms, and metallic entities that produce orthogonal modes. In order to reduce the displacement current between antenna elements, parasitic structures are also employed. In [9, 10], a methodical approach based on Degeneration Mode Theory (DMT) is introduced to enhance MIMO DRA's isolation by generating two orthogonal modes with identical resonance frequencies.

Zhang et al. proposed a MIMO DRA for 5G mm-wave application with enhanced isolation. It resonates at 28 GHz in between 27.5–28.35 GHz, narrow band. This work only describes gain and improved isolation, and does not explain the modes behaviour of DRA [11]. Sahu et al. [12] designed a four-port MIMO DRA having impedance bandwidth 500 MHz. This is a 4 port open feed DRA, resulting in circular polarization, but gain is not much. The modes of DRA are not described. Hu

et al. proposed the MIMO DRA with reduced mutual coupling. They used metal strips on the lateral sides of DRA to change the rotation of E-field, as depicted in paper the 0, 90, 180, and 270 E-field distribution inside the DRA, but the nomenclature of modes is missing [13]. Kiran et al. designed a rectangular DRA with Sierpinski and Minkowski fractals for wideband applications. Two modes are investigated, $TE^{z}_{11\delta}$ and $TE^{z}_{21\delta}$, with 6.74 dBi gain [14]. Tiwari et al. exhibited exceptionally good diversity performance with the three modes TE_{111}, TE_{221}, and TE_{211} [15]. Wang et al. reported TE_{111} at 16 GHz and TE_{131} at 38 GHz frequency. This is a 1×4 DRA array, therefore attains 10 dBi of gain [16]. Fang et al. designed a hollow rectangular DRA with a 180 deg hybrid coupler with the peak gain 6 dBi. It achieves two modes TE_{111} and TE_{113} with 46% impedance bandwidth. Here, DRA is benefited in terms of impedance bandwidth [17]. Fan et al. proposed a dual beam end fire DRA for mm-wave applications. It achieves 6.3 dB of gain with $TE_{12\delta}$ and anti-phase $TE_{13\delta}$ mode and attains 27.6% impedance bandwidth in the proposed antenna [18]. Li et al. proposed a circularly polarized It employs a 2×2 antenna that resonates in the fundamental mode $TE_{11\delta}$ and higher order $TE_{31\delta}$ mode. They explained the E-field distribution at 29 GHz, 32 GHz, 37 GHz, and 39 GHz. Due to the MIMO the antenna achieves 11 dB of measured gain [19]. Cui et al. designed a hybrid DRA with three resonator strips in the frequency band 26.41–30.42 GHz. The proposed 5G bands cover TE_{111} and TE_{131} modes. Cui et al. enable the beam steering capability in their hybrid DRA. The antenna attains the peak gain of 6.8 dB and bandwidth of 12.56% [20]. Finally, Chen and Dong designed a three-port miniaturized DRA for sub-6 GHz 5G frequency band not for 5G frequency band, but $TE_{1\delta1}$, $TE_{1\delta3}$, and $TM_{01\delta}$ modes are observed. This design covers the 360 deg tilt, and units are back-to-back so that the couple between the ports can be suppressed [21].

In this paper, the proposed shape is designed especially for 5G millimeter wave applications which enhances the gain and generates modes. The air vias affect the efficiency but improve the gain and do not interfere in the electric and magnetic fields. It is challenging to provide full coverage because the antenna radiators are orientated in different directions and cannot cover the entire angle range. The low correlation between antenna elements is necessary for a good MIMO antenna. To reduce the mutual coupling between antenna elements, each element must be positioned correctly.

In this proposed work, a cross-shaped four-port MIMO rectangular DRA is designed and fabricated for 5G mm-wave MIMO applications in the range from 22 to 34 GHz. The triple band resonance occurs in this frequency range. The antenna structure is designed in such a way that four RDRAs and four triangle DRAs are merged to form the desired shape operating at the 5G mm-wave frequency band. The proposed DRA placed on the square ground with the length and width of 15 mm. Each element of antenna is fed by a conformal type of microstrip transmission line. By symmetrically locating the four arms at an angle of 90°, the designed antenna generates four directive radiation patterns with the interval of 90° and maintain the peak gain of 8.4 dBi. The $TE_{21\partial}$, $TE_{41\partial}$, $TE_{11\partial}$, $TM_{14\partial}$, and $TM_{41\partial}$ modes are observed at 28.5 GHz resonant frequency for MIMO application. It maintains an efficiency around 74% and low envelope correlation coefficient below 0.0125 for entire band.

2. ANTENNA GEOMETRY AND DESIGN

The present investigation is the first to use simple air vias to improve gain with moderate isolation of mm-wave MIMO DRA. It has been demonstrated by positioning vias inside the single DRA element at an appropriate position, and gain is improved as compared to the previous works. All together, air vias slightly affect the field distribution of the excited antenna without deforming the radiation pattern and keep the main DR radiator same. Furthermore, the loss resulting from air vias is ideally insignificant because the proposed MIMO DR only has one main radiator, and the extra vias do not resonate in the operational band.

A conformal transmission line is used to excite the cross-shaped DRA, which in turn simulates through the proposed ceramic material. With this orientation, fractional bandwidth 19.3% is achieved. The orthogonal alignment of two ports minimizes the mutual coupling value between the ports to less than -15 dB and validates the polarization diversity. The subsequent sections include an explanation of antenna configuration, its investigation, experimental validation, and MIMO parameters.

2.1. Antenna Configuration

The geometry and dimensions of the single element four port dielectric resonator MIMO antenna are displayed in Figure 1 and Table 1. Single cross-shaped DRA of alumina material having relative permittivity of 9.8 is mounted on the roger RT duroid 5880 with loss tangent 0.0009, dielectric constant 2.2, and thickness of 0.254 mm. A conformal fed transmission line is used for exciting the DR from all four directions of the cross shaped DRA (CSDRA). Four vertical air vias are introduced to modify effective dielectric constant of the DR. Thus, the desired modes can be incorporated within one antenna passband.

TABLE 1. Dimensions of the proposed RDRA.

Parameter	Value (in mm)	Parameter	Value (in mm)
Lg	15	fl	2.91
Wg	15	rad	0.2
$Lg = Wp$	10	q	3.4
hs	0.254	b	3
fw	0.6	c	2.41
hd	1.5	d	1.7

Four 50 Ω microstrip feedlines are used for excitation having length ($fl = 2.91$ mm) and width ($fw = 0.6$ mm) along with the four conformal strip length (fl). The dimension of these conformal strips is tailored to improve the antennas performance, and port excitation from microstrip feedline is easily integrated with DRA without creating an air gap. Due to the presence of four ports placed at an equal distance (90° to each other), the designed antenna works as a 4×4 MIMO antenna.

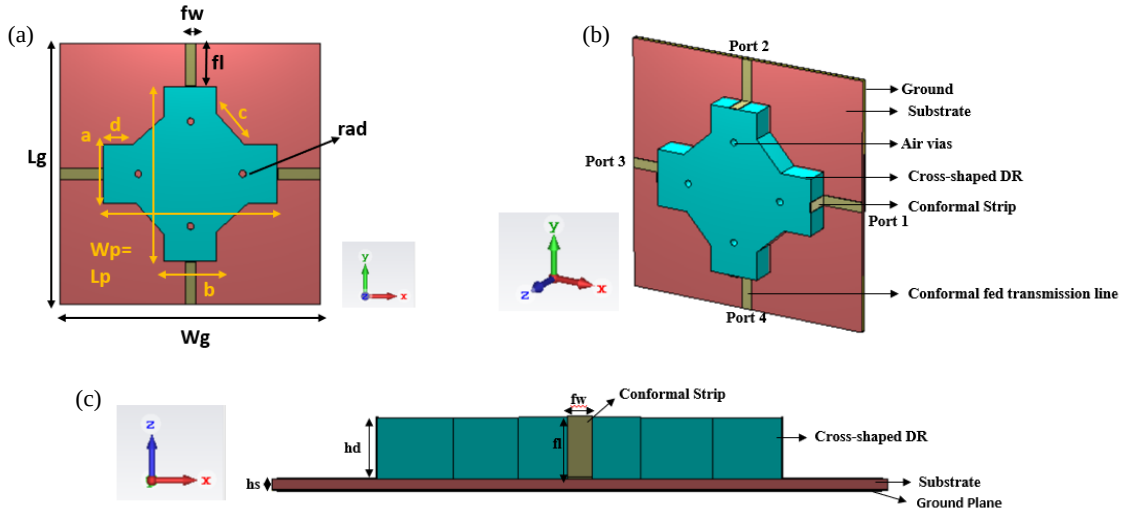

FIGURE 1. Geometrical architecture of the proposed single element MIMO DRA. (a) Front view. (b) 3D view. (c) Side view.

The air vias located at each arm are used for deforming the radiation and slightly affect the field distribution in the excited DR element. Air vias are positioned at an appropriate position in the DRA to get the matched impedance, and losses created by air vias are negligible. The RDRA design is selected to reduce the mutual coupling between various elements and to ensure a low envelope correlation coefficient (ECC) among components that are closely spaced.

The cross-shaped RDRA is attached in the centre of a square substrate in such a way that four conformal fed microstrip lines are used to generate $TE_{21\partial}$, $TE_{41\partial}$, $TE_{11\partial}$, $TM_{14\partial}$, and $TM_{41\partial}$ modes to achieve triple band resonance. All four ports are placed at an equal distance and provide high isolation.

2.2. Parametric Analysis

The key characteristics of the antenna may be simulated to provide a summary of the design process. The main objective of this parametric study is to examine the relationships between the important parameters and the resonance frequencies along with determinate variables.

In this section, parametric analysis is carried out to characterise the 4×4 MIMO DRA. First, the effects of height of the proposed DRAs with single port and with four ports are shown in Figures 2(a) & 2(b) and explained. Figure 2(a) shows the variation of S-parameter due to the change in the height of DRA keeping length and width of each arm fixed as per the operating frequency. It is observed that for d varied from 1 mm to 5 mm, the resonant frequency is approximately shifted to the upper and lower side bands, but the antenna does not resonate exactly at 28.5 GHz with single port. With four ports, at $d = 1.5$ mm, the proposed antenna resonates at 28.5 GHz in the band between 25 and 30 GHz.

Next, the effects of different heights of the substrate on the proposed DRA are investigated as depicted in Figure 2(b). Practically, only a few substrate heights are available by the Roger laminates manufacturing, i.e., 0.127 mm, 0.254 mm, 0.508 mm, 0.787 mm, 1 mm, and 1.575 mm. It is noted that at $hs = 0.254$ mm, the reflection coefficient $|S_{11}|$ exactly resonates in 5G mm-wave band with improved gain among all other substrate heights as shown in Figure 2(c).

For efficient impedance matching, the length and width of the feedline has to be optimized, illustrated in Figure 2(c). Feeding width (Fw) is an essential characteristic for DRA excitation because it enables coupling between the DRA and conformal fed microstrip line. At $Fw = 0.6$ mm, the antenna resonates perfectly at 28.5 GHz frequency with 14% impedance bandwidth and at $Fw = 0.8$ and 1 mm, and frequency shifts to 30 GHz, but it offers 10 GHz of wide bandwidth.

2.3. Mode Analysis

For the proposed DRA, the $TE_{mn\delta}$ mode is excited along z-direction. Since the $TE_{mn\delta}$ mode is excited along z-direction, $E_z = 0$. Thus, $\vec{E}_{xy}$ and $\vec{H}_{xy}$ are given as Equations (1) & (2)

$$\vec{H}_{xy} = -\frac{jk_z}{k_c^2}\nabla_t H_z \tag{1}$$

$$\vec{E}_{xy} = -\frac{\omega\mu_0}{k_z}\hat{a}_z \times \vec{H}_{xy} \tag{2}$$

By using the Marcatili's approximation technique for a rectangular coordinate system as illustrated in the investigation paper by Mongia and Bhartia [3], H_z field components depend on even or odd values of "m" and "n", which are given by Equations (3) and (4):

$$H_z = \cos(k_x x)\cos(k_y y) \quad (\text{If } m \text{ and } n \text{ are odd}) \tag{3}$$

$$H_z = \sin(k_x x)\cos(k_y y) \quad (\text{If } m \text{ even and } n \text{ odd}) \tag{4}$$

By substituting Equations (3) and (4) in (1) and (2), all field components (E&H) for $TE_{mn\delta}$ modes are calculated and stated in the subsequent equations:

$$E_x = Ak_y \cos(k_z z) \begin{Bmatrix} \sin(k_y y) \\ \cos(k_y y) \end{Bmatrix} \begin{Bmatrix} \cos(k_x x) \\ \sin(k_x x) \end{Bmatrix} \tag{5}$$

$$E_y = -Ak_x \cos(k_z z) \begin{Bmatrix} \cos(k_y y) \\ \sin(k_y y) \end{Bmatrix} \begin{Bmatrix} \sin(k_x x) \\ \cos(k_x x) \end{Bmatrix} \tag{6}$$

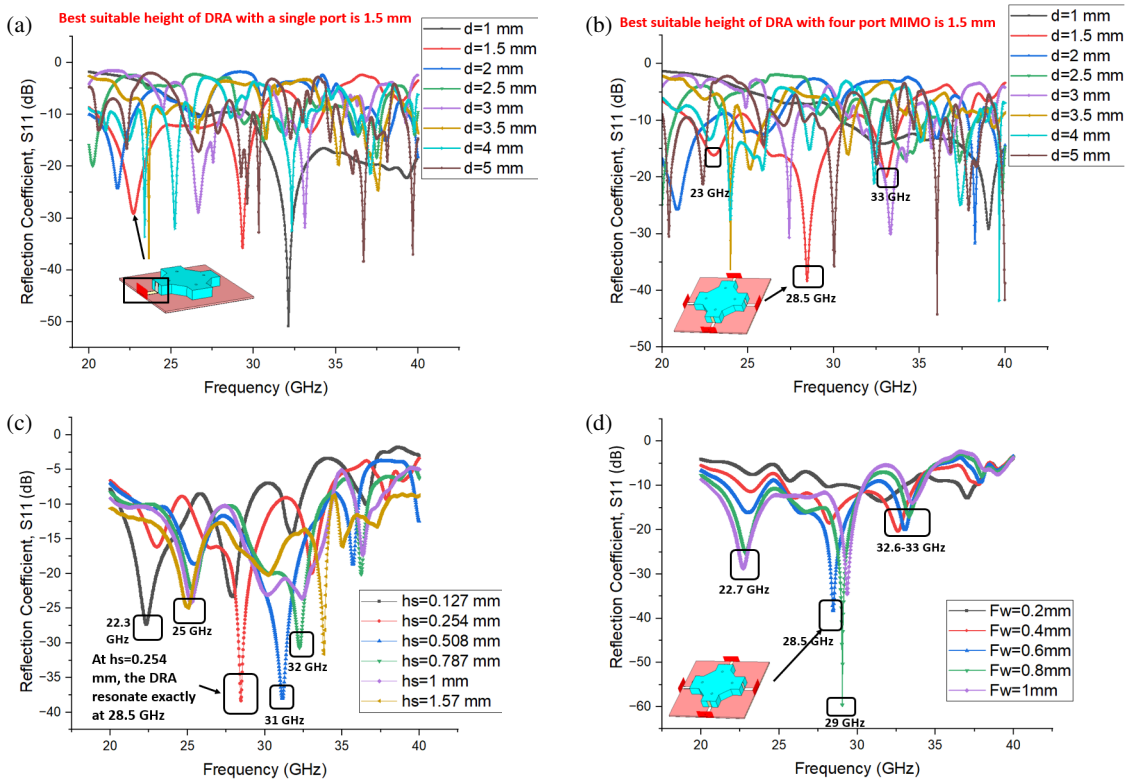

FIGURE 2. (a) Parametric simulated reflection coefficient at different heights of DRA with single port, (b) parametric simulated reflection coefficient at different heights of DRA with four ports, (c) parametric simulated reflection coefficient at different heights of substrate, (d) parametric simulated reflection coefficient at different feed widths.

$$E_z = 0 \tag{7}$$

$$H_x = A\frac{k_x k_z}{j2\pi\mu f_{mn}} \sin(k_z z) \begin{Bmatrix} \cos(k_y y) \\ \cos(k_y y) \end{Bmatrix} \begin{Bmatrix} \sin(k_x x) \\ \cos(k_x x) \end{Bmatrix} \tag{8}$$

$$H_y = A\frac{k_y k_z}{j2\pi\mu f_{mn}} \sin(k_x x) \begin{Bmatrix} \sin(k_y y) \\ \cos(k_y y) \end{Bmatrix} \begin{Bmatrix} \cos(k_x x) \\ -\sin(k_x x) \end{Bmatrix} \tag{9}$$

$$H_z = A\frac{k_x^2 + k_y^2}{j2\pi\mu f_{mn}} \cos(k_z z) \begin{Bmatrix} \cos(k_x x) \\ \sin(k_x x) \end{Bmatrix} \begin{Bmatrix} \cos(k_y y) \\ \cos(k_y y) \end{Bmatrix} \tag{10}$$

where the lower functions are selected if m is even, and n is odd, while the upper functions are selected if the associated values of m and n are odd.

The RDRA is modelled by Dielectric Waveguide Model (DWM) in order to predict resonating modes of the proposed DRA at the targeted resonating frequencies. The resonant frequency f_{mn} of the mode $TE_{mn\partial}$ can be predicted by using transcendental equations:

$$k_x \tan\left(\frac{k_x d}{2}\right) = \sqrt{(\varepsilon_r - 1)k_{mn}^2 - k_x^2} \tag{11}$$

where,

$$k_{mn} = \frac{2\pi f_{mn}}{c}, \quad k_y = m\frac{\pi}{w}, \quad k_z = n\frac{\pi}{b},$$

and $\quad k_x^2 + k_y^2 + k_z^2 = \varepsilon_r k_{mn}^2$

and the speed of light is designated as c. The various E- and H-field modes within the RDRA are calculated by using Equations (5)–(10).

Figure 3 shows the normalized E-field for the one fundamental and three higher order modes particularly at 28.5 GHz, because maximum resonance occurs at this frequency from all the four ports. These field configurations exist inside the RDRA and approximated by the magnetic dipoles. From Figure 3(a) and with the help of field equations, the modes that exist are: $TE_{21\partial}$ mode that is observed at 28.5 GHz frequency when port 1 is excited, and in these two full cycles of field variation is depicted. The $TE_{41\partial}$ mode is observed at 28.5 GHz frequency when port 2 and port 4 are excited and in these four cycles are observed in Figures 3(b), (d). Referring to Figure 3(c), the fundamental mode $TE_{11\partial}$ is observed only when port 3 is excited. These fields are calculated through the x-y region. Similarly, when magnetic fields are excited within RDRA, the two modes, $TM_{14\partial}$ from ports 1 and 3 and $TE_{41\partial}$ from ports 2 and 4, are observed at frequency 28.5 GHz, where "δ" is specified as the function of a half-cycle of the field variation. These fields can be observed in Figures 4(a), (b), (c), (d). Using transient solver, the entire research was conducted in Computer Simulation Technology (CST) Microwave Studio.

3. SIMULATION AND MEASURED RESULTS

To verify the proposed design, a prototype of the proposed 4×4 MIMO RDRA is fabricated by using printed circuit board

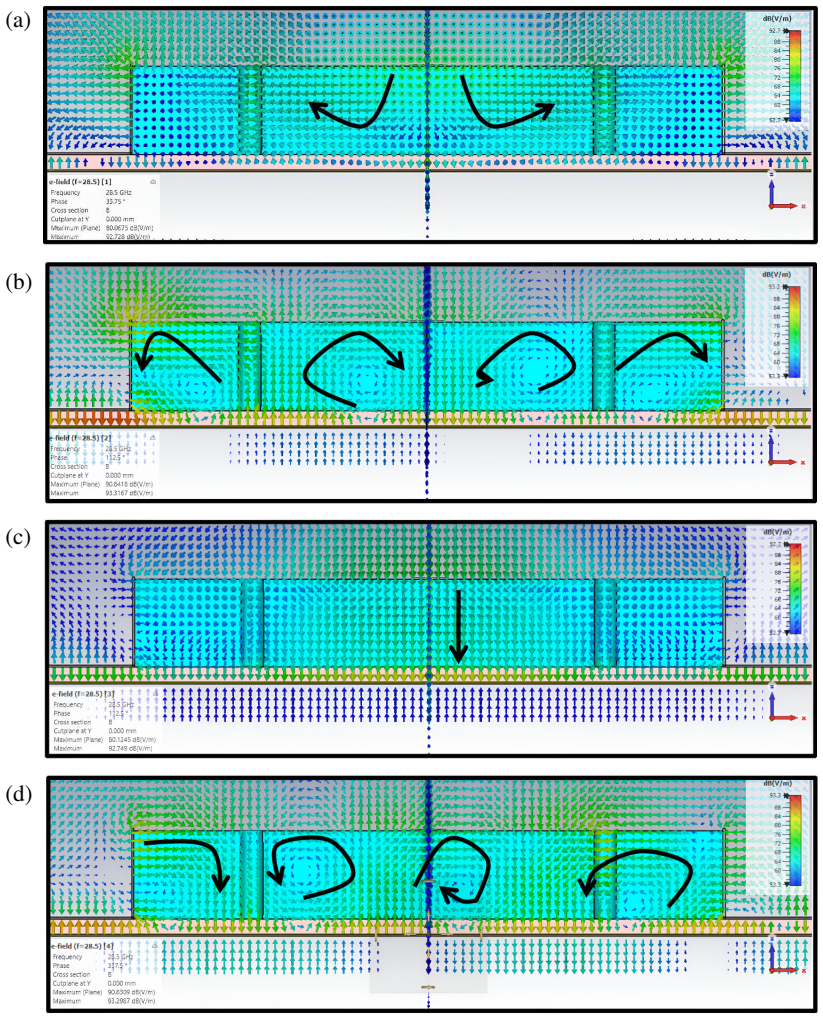

FIGURE 3. E-field distribution on DR surface: (a) $TE_{21\delta}$ mode at 28.5 GHz frequency from port 1, (b) $TE_{41\partial}$ mode at 28.5 GHz frequency from port 2, (c) $TE_{11\partial}$ mode at 28.5 GHz frequency from port 3, and (d) $TE_{41\partial}$ mode at 28.5 GHz frequency from port 4.

(PCB) manufacturing process and tested in a 40 GHz anechoic chamber. Figure 5 shows the manufacturing process of DR by alumina crucibles, and Figure 6 shows the fabricated model of the proposed RDRA. The dielectric constant of alumina is 9.9, and it is an easily available material. Only the feeding strips are imprinted on PCB. Copper conformal strips were directly pasted on the DRA, and DRA is pasted onto the substrate. All the dimensions of the proposed DRA are the same as in Figure 1.

In the proposed prototype, the dielectric resonator is fixed by a thin layer of adhesive on the substrate. By using epoxy glue, the dielectric constant is in between 2 and 4, and loss tangent (0.001–0.02) must be accounted for EM simulations and design that affects the resonant frequency, Q-factor, and field distribution. S-parameters of the DRA are measured with the help of an N523A vector network analyser (VNA) by Agilent Technologies as shown in Figure 7(a), and the setup of DRA inside the anechoic chamber is shown in Figure 7(b). The slight discrepancy noticed in response is due to application of adhesive that is responsible for securing the ceramic onto the roger substrate. It can also be due to biasing lines.

Figures 8(a), (b), (c), & (d) depict the simulated and measured reflection coefficient plots. The simulated impedance bandwidth is 14% (26–30 GHz) for $|S_{11}|$, $|S_{33}|$ and 15% (25–30 GHz) for $|S_{22}|$, $|S_{44}|$, while the measured impedance bandwidth is 15.789% (26–30.5 GHz) for $|S_{11}|$, $|S_{33}|$ and 16.789% (25–30.5 GHz) for $|S_{22}|$, $|S_{44}|$. The 25–30 GHz frequency band is acceptable for 5G millimeter wave applications.

In order to minimize multipath fading, 5G applications need a minimum of four antenna ports. As a result, single port antenna is transformed into a four port MIMO antenna. Converting a single port into four port MIMO antenna may often be done in two ways: Four ports can be arranged (i) in parallel or antiparallel configuration, or (ii) orthogonally. The ground plane of every antenna port is either common or linked in the scenarios. It is required for the design of MIMO antennas. Because of orthogonal coupling of ports and increased size of ground plane, it can be observed that the isolation of the proposed DRA is below -15 dB. Isolation in MIMO antenna systems is the degree to which one antenna element is electrically separated from the others (decoupled). A high degree of isolation reduces mutual connection. The transmission coefficient

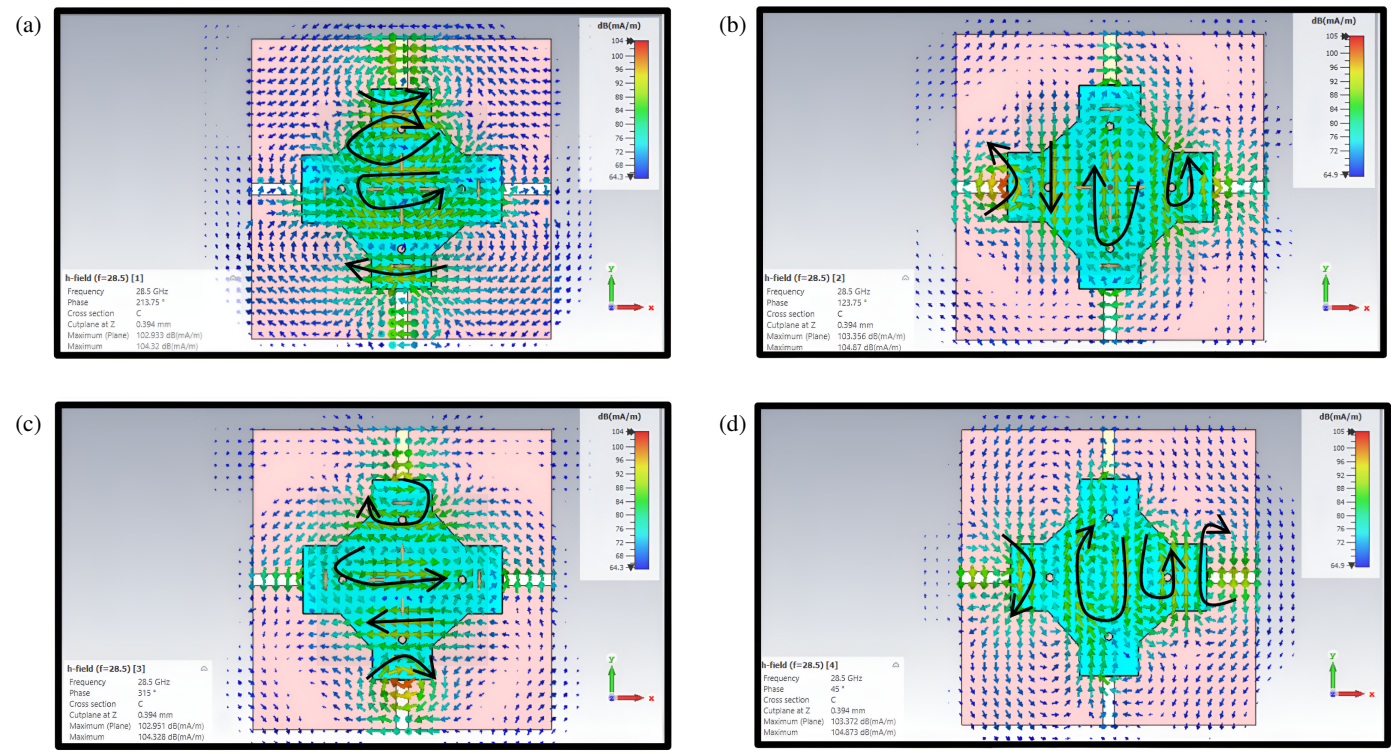

FIGURE 4. H-field distribution on DR surface: (a) $TM_{14\delta}$ mode at 28.5 GHz frequency from port 1, (b) $TM_{41\partial}$ mode at 28.5 GHz frequency from port 2, (c) $TM_{14\partial}$ mode at 28.5 GHz frequency from port 3, and (d) $TM_{41\partial}$ mode at 28.5 GHz frequency from port 4.

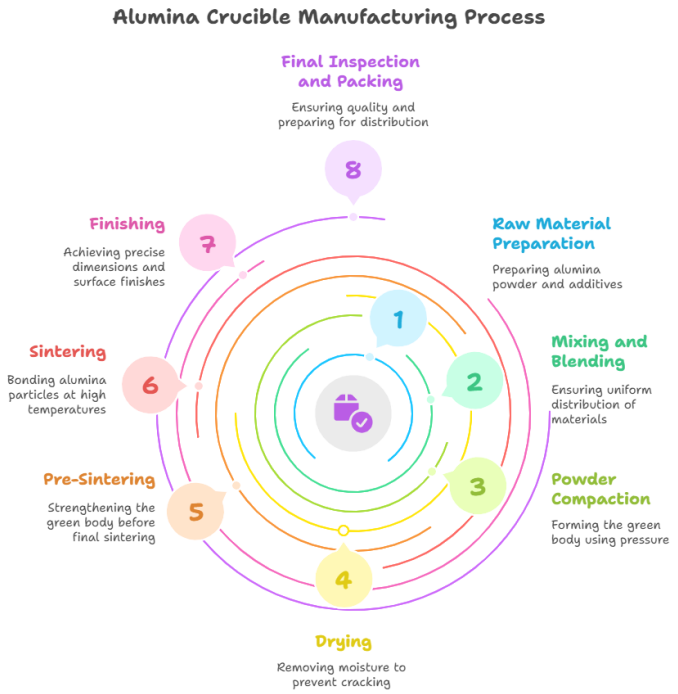

FIGURE 5. Dielectric resonator antenna manufacturing process.

between two antenna ports is represented by parameters S_{21}, S_{31}, and S_{41}. Good isolation is indicated if $S < -20$ dB, whereas satisfactory isolation is indicated if $S < -15$ dB. S_{21} and S_{41} in the proposed design have acceptable isolation levels of less than -15 dB as shown in Figures 8(e), (f), (g).

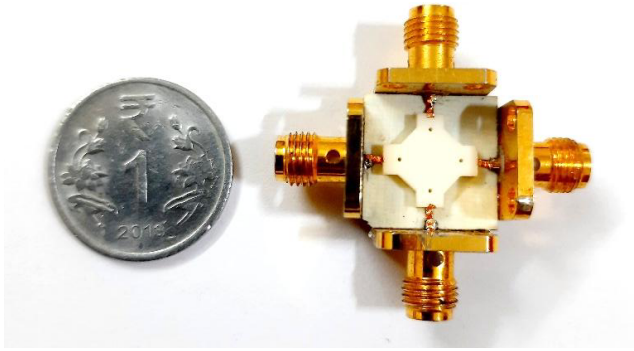

FIGURE 6. Fabricated model of the proposed MIMO DRA.

There is a good agreement between measured and simulated responses. Therefore, the overall inter-element isolation performance is satisfactory for the proposed four element MIMO antenna.

Figure 9 depicts the compared response of simulated and measured gains of proposed antenna. The two-antenna method is used for gain measurement in a closed anechoic chamber. Measured value is 0.1 dBi gain lesser than the simulated one that is 8.4 dBi gain achieved in simulation and 8.3 dBi gain attained within operating bandwidth via measurement. The proposed antenna offers 74% radiation efficiency at 28.5 GHz.

Figure 10 represents far-field analyses at the resonating frequency that signifies the radiation propagation level from each port when it gets excited. It also shows the electromagnetic field distribution pattern at each resonating frequency. The radiation patterns for each port of the MIMO antenna system

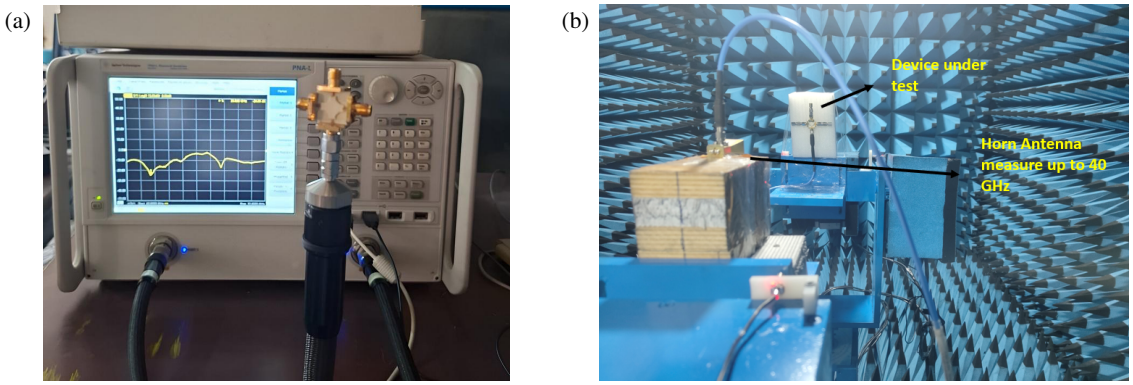

FIGURE 7. (a) Antenna measurement by VNA. (b) Antenna front view inside anechoic chamber DUT.

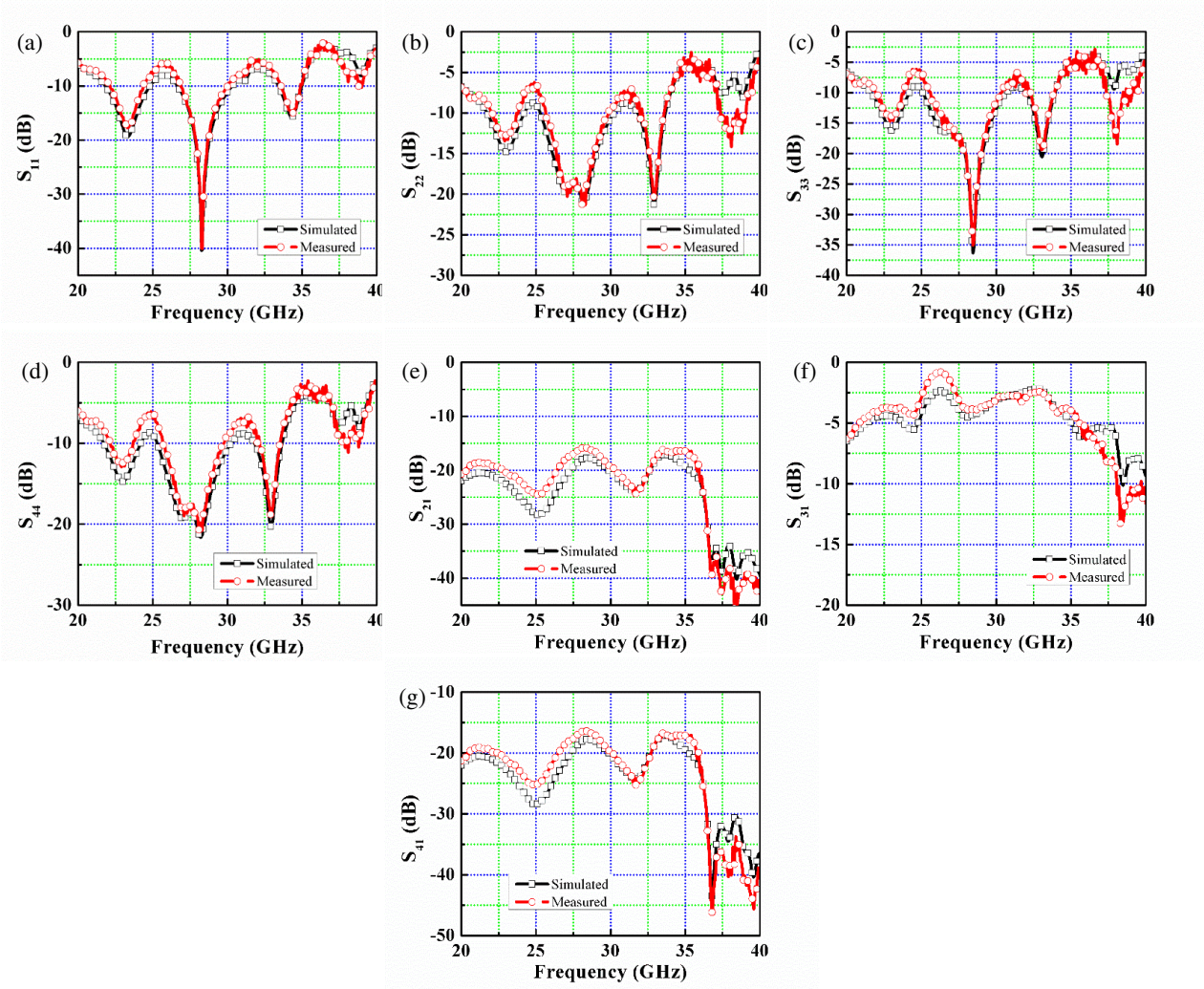

FIGURE 8. Simulated and measured S-parameters of the proposed 4×4 MIMO DRA (a) S_{11}, (b) S_{22}, (c) S_{33}, (d) S_{44}, (e) S_{21}, (f) S_{31}, (g) S_{41}.

show a horn like orientation. This indicates that the dielectric resonators' main beams, which produce the radiation, are pointed in opposite directions. It also depends on the active port position. If port 1 is active, other are in passive mode, and in this case the beam is directed in forward direction and vice versa.

The proposed DRA displays radiation pattern in different directions. This radiation pattern maintains a good coverage area and enhances diversity. The radiation pattern is measured in an anechoic chamber at 28.5 GHz. The simulated and measured co-polarization and cross-polarization responses are displayed in Figure 11. It can be observed that cross-polarization response

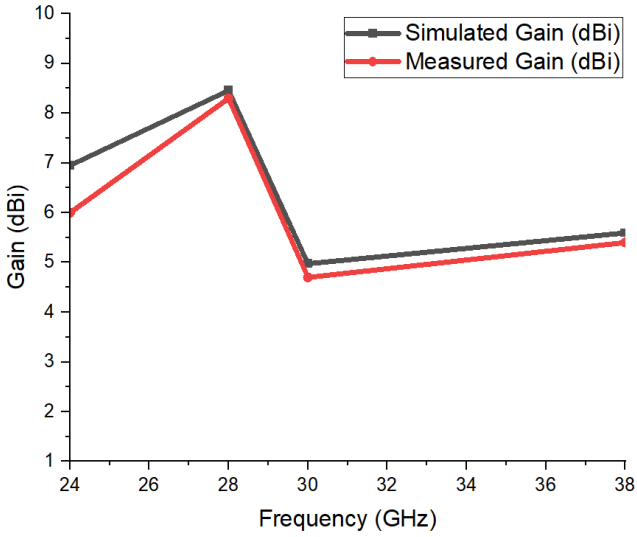

FIGURE 9. The compared simulated and measured gain responses of the proposed single element MIMO DRA.

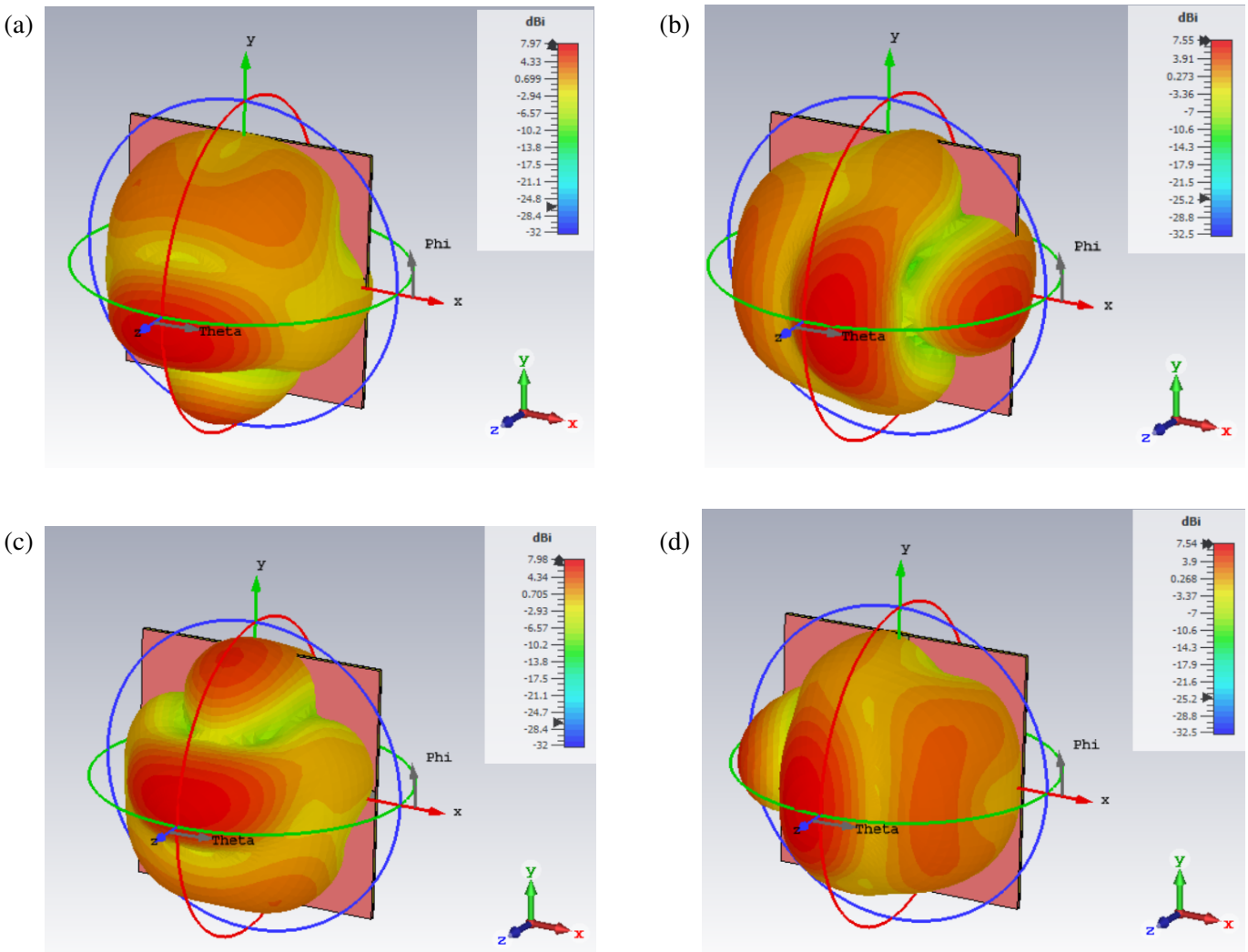

FIGURE 10. Simulated far-field analysis at 28.5 GHz of frequency, (a) from port 1, (b) from port 2, (c) from port 3, and (d) from port 4.

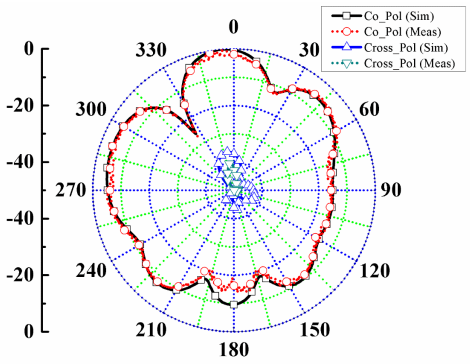

FIGURE 11. The compared simulated and measured co-polarization and cross-polarization responses at 28.5 GHz.

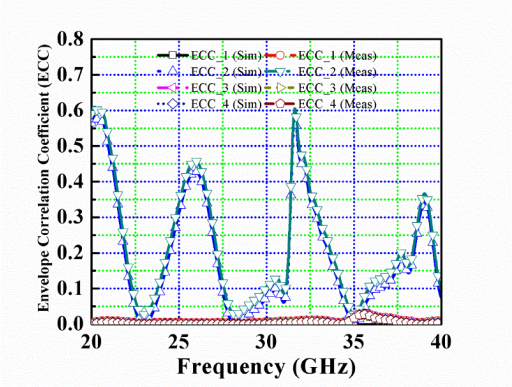

FIGURE 12. ECC of the presented MIMO DRA.

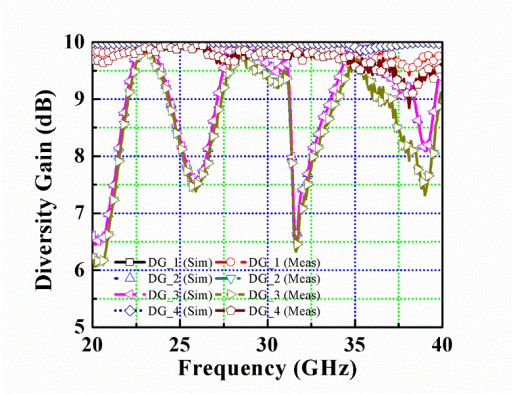

FIGURE 13. DG of the presented MIMO DRA.

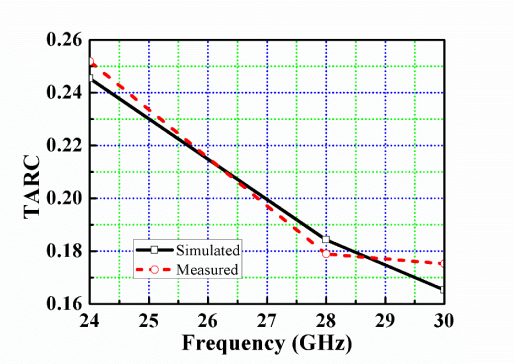

FIGURE 14. Comparison of measured and simulated co-polarization and cross-polarization responses.

is lower than co-polarization response, and it is quite good for antenna performance. The connectors in the DRA are the cause of the difference between the simulated and measured values. The detected radiation pattern is also impacted by the testing cable.

Two significant parameters influence the antenna design in the investigation of MIMO antennas. The correlation among the ports is represented by envelope correlation coefficient (ECC). In MIMO antenna systems, ECC, which regulates interactions between antenna variables according to individual characteristics, is a crucial component. ECC should ideally be zero, which denotes that there is no coupling between radiating elements. For a MIMO system to function well, the ECC must be less than 0.5. The four port MIMO antenna S-parameters are used to calculate ECC by equation:

$$ECC = \frac{\left|S_{11}^{*}S_{12}^{*} + S_{21}^{*}S_{22}^{*} + S_{13}^{*}S_{32}^{*} + S_{14}^{*}S_{42}^{*}\right|^{2}}{\left(1 - \left|S_{11}\right|^{2} - \left|S_{21}\right|^{2} - \left|S_{31}\right|^{2} - \left|S_{41}\right|^{2}\right)\left(1 - \left|S_{12}\right|^{2} - \left|S_{22}\right|^{2} - \left|S_{32}\right|^{2} - \left|S_{42}\right|^{2}\right)} \quad (12)$$

where $*$ is the Hermitian product operator of reflection and transmission coefficients of the MIMO antenna. ECC indicates how much strength of radiation fields from each port interacts with the others, and its value should be less than 0.2 within the intended frequency of operation for optimal MIMO system performance. For efficient MIMO DRA, it should be less than 0.2. Figure 12 presents the simulated and measured variation responses of ECC with frequency, and due to the symmetry in design, ECCs for all the four port are almost the same which is 0.0125.

In MIMO DRA systems, diversity gain (DG) is essential because it measures the impact of utilizing diversity techniques on the transmitted power. It is computed by equation:

$$DG = 10\sqrt{\left(1 - \left|ECC\right|^{2}\right)} \quad (13)$$

The highest apparent diversity gain at the 1% rate is 10. The DG depends on ECC by Formula (13). If DG is closer to 10, then it ensures that the proposed DRA MIMO antenna will perform better in terms of diversity. For the proposed MIMO RDRA, Figure 13 shows that the simulated and measured values of DG are greater than 9.7 dB and 9.8 dB (almost 10 dB), respectively.

Another MIMO parameter is total active reflection coefficient (TARC) which is the parameter used to characterize multiport in MIMO antenna systems and array antennas. It is dependent on the frequency and also depends on the tapering and scan angles. Here, TARC is represented in terms of frequency as shown in Figure 14.

The measured TARC of proposed antenna is 0.18 which means -14.9 in dB. This implies that the reflected total incident power is 3.24%, and the rest 96.8% is radiated, which is very good for a MIMO antenna system. This proves that there is an excellent matching among all the ports when theyare excited simultaneously and signifies a well-matched and efficient radiator MIMO DRA suitable for 5G mm-wave communication.

TABLE 2. Comparison of the proposed work with the previous work.

Ref.	Author's Name & Published Year	Operating Frequency (GHz)	Size of Radiating element (mm^3)	Imp. BW. (%)	Gain (dB)	No. of elements	Observed Modes	Isolation (dB)	ECC
[11]	Yin Zhang, 2019	27.5–28.3	$9.5 \times 7.5 \times 2.54$	2.8	8	2×2	TE^{y}_{311}	24	0.013
[12]	Sahu, 2022	27.4–28.4	$9 \times 2 \times 1$	4.2	6.3	1	TE^{y}_{111}	18.3	0.09
[22]	Yan Ting Liu, 2023	22.5–30	$3.24 \times 4.78 \times 0.83$	21.6	8	4×4	$TE^{y}_{3\delta1}$, $TE^{y}_{1\delta1}$	20	—
[20]	Lun-Xue Cui, 2023	26.4–30.4/39	$2.25 \times 0.7 \times 0.4$	14.11	7.3	1	TE_{111}, TE_{131}	—	—
[16]	Ya-Xing Wang, 2023	13.3–19/36.3–40	$6 \times 6 \times 3.8$	9.7	10.6/14.3	1×4	TE_{111}, TE_{131}	—	—
[15]	Poonam Tiwari, 2024	24–32	$6.5 \times 5 \times 2.45$	11.6	8	4×4	TE_{111}, TE_{221}, TE_{211}	27	0.0006
[19]	Jianxing Li, 2024	28/38	$2.6 \times 2.6 \times 0.88$	35.6	11.7	1×4	$TE_{11\delta}$, $TE_{31\delta}$	—	—
[18]	Gonghao Fan, 2025	24.6	$3.25 \times 9.25 \times 0.63$	27.6	6.3	1	$TE_{11\delta}$, $TE_{12\delta}$, $TE_{13\delta}$	—	—
This work	**G. Sharma, 2025**	**28.5 (26–30)**	**$10 \times 10 \times 1.5$**	**14**	**8.4**	**1**	**$TE_{21\delta}$, $TE_{41\delta}$, $TE_{11\delta}$, $TM_{14\delta}$ and $TM_{41\delta}$**	**15**	**0.0125**

4. COMPARISON OF THE PROPOSED WORK WITH THE PREVIOUS WORKS

A comparison of the 4×4 MIMO DRA design with existing DRA is specified in Table 2. As the table illustrates, our design features triple bands with good gain and good ECC value amongst all of the DRA designs. A thorough performance comparison between the proposed antenna and earlier research is shown in Table 2. Compared to previous research efforts, the offered data demonstrates major innovations brought about by the suggested antenna, demonstrating notable improvements in operating frequency, impedance bandwidth, gain, number of radiating elements, observed modes, and ECC. Since our antenna size is compact and deploys with low dielectric constant material, after manufacturing of the proposed antenna, it is quite appealing for real-world applications.

5. CONCLUSION

In this proposed work, a novel single element four port MIMO DRA with triple bands, enhanced gain, and acceptable isolation for 5G mm-wave application is constructed, evaluated, and measured. It generates four directional radiation patterns and yields good diversity. The elements are arranged in a square ground plane of length and width of 15 mm in such a way that each element radiates in all four directions resulting in minimum field correlation. The functioning of DRA can be controlled by the combination of DRA and air vias structure. The air vias have been utilized to control input impedance, allowing for adjustment of the DRA's bandwidth and radiation performance. The DRA is fabricated with low-loss ceramic material, attached to the substrate with conformal fed transmission line and measured in an anechoic chamber. Using the proposed design technique, 8.4 dBi gain is achieved with 74% radiation efficiency. The proposed DRA achieves triple bands and -15 dB isolation throughout the band. The communication parameter envelope correlation coefficient is 0.0125, and diversity gain is 9.8 dB. The achieved measured responses are in a good agreement with simulated response. Hundreds of antennas operating at low latency (less than microseconds) are required at this frequency range in order to support wireless communication, with a particular focus on internet gadgets. This prompted scientists to keep producing such work involving millimeter waves applications.

REFERENCES

[1] Soren, D., R. Ghatak, R. K. Mishra, and D. Poddar, "Dielectric resonator antennas: Designs and advances," *Progress In Electromagnetics Research B*, Vol. 60, 195–213, 2014.

[2] Petosa, A., *Dielectric Resonator Antenna Handbook*, Artech House, 2007.

[3] Mongia, R. K. and P. Bhartia, "Dielectric resonator antennas — A review and general design relations for resonant frequency and bandwidth," *International Journal of Microwave and Millimeter-Wave Computer-Aided Engineering*, Vol. 4, No. 3, 230–247, 1994.

[4] Sharawi, M. S., S. K. Podilchak, M. U. Khan, and Y. M. Antar, "Dual-frequency DRA-based MIMO antenna system for wireless access points," *IET Microwaves, Antennas & Propagation*, Vol. 11, No. 8, 1174–1182, 2017.

[5] Sharawi, M. S., M. U. Khan, A. B. Numan, and D. N. Aloi, "A CSRR loaded MIMO antenna system for ISM band operation," *IEEE Transactions on Antennas and Propagation*, Vol. 61, No. 8, 4265–4274, Aug. 2013.

[6] Anab, M., M. I. Khattak, S. M. Owais, A. A. Khattak, and A. Sultan, "Design and analysis of millimeter wave dielectric resonator antenna for 5G wireless communication systems," *Progress In Electromagnetics Research C*, Vol. 98, 239–255, 2020.

[7] Pan, Y. M., X. Qin, Y. X. Sun, and S. Y. Zheng, "A simple decoupling method for 5G millimeter-wave MIMO dielectric resonator antennas," *IEEE Transactions on Antennas and Propagation*, Vol. 67, No. 4, 2224–2234, Apr. 2019.

[8] Yan, J.-B. and J. T. Bernhard, "Design of a MIMO dielectric resonator antenna for LTE femtocell base stations," *IEEE Transactions on Antennas and Propagation*, Vol. 60, No. 2, 438–444, Feb. 2012.

[9] Murthy, N., "Improved isolation metamaterial inspired mm-Wave MIMO dielectric resonator antenna for 5G application," *Progress In Electromagnetics Research C*, Vol. 100, 247–261, 2020.

[10] Al-Falajy, N. and O. Y. K. Alani, "Design considerations of ultra dense 5G network in millimeter wave band," in *2017 Ninth International Conference on Ubiquitous and Future Networks (ICUFN)*, 141–146, Milan, Italy, 2017.

[11] Zhang, Y., J.-Y. Deng, M.-J. Li, D. Sun, and L.-X. Guo, "A MIMO dielectric resonator antenna with improved isolation for 5G mm-wave applications," *IEEE Antennas and Wireless Propagation Letters*, Vol. 18, No. 4, 747–751, Apr. 2019.

[12] Sahu, N. K., G. Das, R. K. Gangwar, and K. Rambabu, "An arrangement for four-element MIMO DRA with complementary CP diversity," *IEEE Antennas and Wireless Propagation Letters*, Vol. 20, No. 9, 1616–1620, Sep. 2021.

[13] Hu, Y., Y. M. Pan, and M. D. Yang, "Circularly polarized MIMO dielectric resonator antenna with reduced mutual coupling," *IEEE Transactions on Antennas and Propagation*, Vol. 69, No. 7, 3811–3820, Jul. 2021.

[14] Kiran, D. V., D. Sankaranarayanan, and B. Mukherjee, "Compact embedded dual-element rectangular dielectric resonator antenna combining sierpinski and minkowski fractals," *IEEE Transactions on Components, Packaging and Manufacturing Technology*, Vol. 7, No. 5, 786–791, May 2017.

[15] Tiwari, P., J. K. Rai, V. Gahlaut, and P. Ranjan, "Compact quad element dual band high gain MIMO rectangular dielectric resonators antenna for 5G millimeter wave application," *AEU — International Journal of Electronics and Communications*, Vol. 178, 155280, 2024.

[16] Wang, Y.-X., Z. Chen, and T. Yuan, "Design of a dual-band dielectric resonator antenna array for millimeter-wave communication," *IEEE Antennas and Wireless Propagation Letters*, Vol. 22, No. 9, 2190–2194, Sep. 2023.

[17] Fang, X. S., K. P. Shi, and Y. X. Sun, "Design of the single-/dual-port wideband differential dielectric resonator antenna using higher order mode," *IEEE Antennas and Wireless Propagation Letters*, Vol. 19, No. 9, 1605–1609, Sep. 2020.

[18] Fan, G., W. Qin, Y. Guo, J. Shi, and R. Jiang, "Millimeter-wave wideband dual-beam end-fire dielectric resonator antenna," *IEEE Antennas and Wireless Propagation Letters*, Vol. 24, No. 3, 671–675, Mar. 2025.

[19] Li, J., X. Yu, S. Gao, C. Li, S. Yan, and K.-D. Xu, "Wideband circularly polarized substrate integrated dielectric resonator antenna array for 5G millimeter-wave applications," *IEEE Antennas and Wireless Propagation Letters*, Vol. 23, No. 12, 4378–4382, Dec. 2024.

[20] Cui, L.-X., X.-H. Ding, W.-W. Yang, L. Guo, L.-H. Zhou, and J.-X. Chen, "Communication compact dual-band hybrid dielectric resonator antenna for 5G millimeter-wave applications," *IEEE Transactions on Antennas and Propagation*, Vol. 71, No. 1, 1005–1010, Jan. 2023.

[21] Chen, Z. and Y. Dong, "A self-decoupled miniaturized wideband tri-port pattern diversity dielectric resonator antenna," *IEEE Antennas and Wireless Propagation Letters*, Vol. 23, No. 12, 4213–4217, Dec. 2024.

[22] Liu, Y.-T., B. Ma, S. Huang, S. Wang, Z. J. Hou, and W. Wu, "Wideband low-profile connected rectangular ring dielectric resonator antenna array for millimeter-wave applications," *IEEE Transactions on Antennas and Propagation*, Vol. 71, No. 1, 999–1004, Jan. 2023.